Proc. Natl. Acad. Sci. USA
Vol. 86, pp. 8602–8606, November 1989
Geophysics

Search for deep slabs in the Northwest Pacific mantle

(subduction/lithosphere/residual spheres/lower mantle)

HUA-WEI ZHOU AND DON L. ANDERSON

Seismological Laboratory, California Institute of Technology, Pasadena, CA 91125

Contributed by Don L. Anderson, August 10, 1989

ABSTRACT **A residual sphere is formed by projecting seismic ray travel-time anomalies, relative to a reference Earth model, onto an imaginary sphere around an earthquake. Any dominant slab-like fast band can be determined with spherical harmonic expansion. The technique is useful in detecting trends associated with high-velocity slabs beneath deep earthquakes after deep-mantle and near-receiver effects are removed. Two types of corrections are used. The first uses a tomographic global mantle model; the second uses teleseismic station averages of residuals from many events over a large area centered on the events of interest. Under the Mariana, Izu-Bonin, and Japan trenches, the dominant fast bands are generally consistent with seismicity trends. The results are unstable and differ from the seismicity trend for Kurile events. The predominant fast band for most deep earthquakes under Japan is subhorizontal rather than near vertical. We find little support for the deep slab penetration hypothesis.**

Analyses of residual spheres (RS)—i.e., focal sphere projections of travel time residuals or anomalies—of some subduction zone earthquakes in the NW Pacific gave steeply dipping slab-like fast arrival patterns, assumed to be caused by high-velocity lithospheric slabs penetrating deep into the lower mantle (1–3). However, Zhou *et al.* (4) found strong effects from diffuse anomalies in the deep mantle and near the receivers, far from the source region, that can be mistaken for near-source slab signatures. They also found flat-lying fast patterns in the blind zones of previous studies. We refer to the cumulative travel time effect caused by inhomogeneities in the deep mantle (deeper than 1500 km for downgoing rays) and receiver mantle (for upgoing teleseismic rays) as teleseismic effects, to distinguish them from the near-source slab effect. The present paper uses a fitting technique to detect slab-like fast trends in observed RS after corrections are applied to remove teleseismic effects.

DATA AND CORRECTIONS

We use 33 events (Fig. 1) from the NW Pacific, numbered as in ref. 4. The data are P-wave travel times (5). Data processing includes removal of a global residual average (6) at each station, a correction for Earth's ellipticity (7), source relocation, and discarding data with Jeffreys–Bullen (JB) residuals exceeding 6 s, after travel times computed for the JB model are subtracted from the observations.

Evidence of significant teleseismic or non-near-source effects was illustrated in ref. 4 in two ways. First, the prediction from a mantle P-wave velocity model (6) shows that the region immediately below the deepest earthquakes, depths 650–1500 km, has an effect comparable to or smaller than the effect of the deep mantle and receiver upper mantle. Second, the average residuals from several dozen of the best-recorded events in the NW Pacific at teleseismic stations were calculated. These station residual averages represent a cumulative contribution from long-wavelength anomalies in regions far from the source, since the rays converge toward the teleseismic stations. A RS constructed from these average residuals (similar to Fig. 2), however, has a distinctive slab-like pattern. That is to say, deep-mantle effects, when projected onto a RS for a given earthquake, sometimes mimic, and can be mistaken for, the effect of a slab.

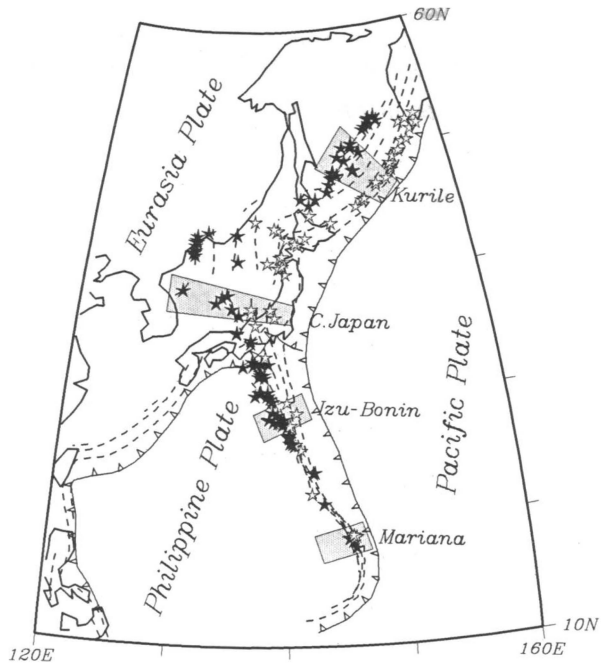

FIG. 1. The major NW Pacific subduction zones are shown by contours at 100-km depth intervals. Stars are earthquakes (4), and solid ones are deeper than 300 km. Those in the shaded areas are used in this study.

Two methods of correction are used to remove non-near-source travel-time effects. In the first we use tomographic models of the mantle. In the second we use station averages that are constructed by using the regional events. Creager and Jordan (3) corrected for the effects of the lower-mantle model of Dziewonski (8), but they conclude that the correction is minor. Dziewonski (8) concluded, however, that the real variations may be significantly larger. His method of smoothing and damping underestimates the total model variation. The Clayton–Comer (6) velocity model used in ref. 4 has both short- and long-wavelength components and also extends up to the receivers. In this paper the Clayton–Comer model is used in the first type of teleseismic correction. Travel times calculated from 1500 km depth to the receiver are removed from the data.

The publication costs of this article were defrayed in part by page charge payment. This article must therefore be hereby marked "*advertisement*" in accordance with 18 U.S.C. §1734 solely to indicate this fact.

Abbreviation: RS, residual sphere(s).

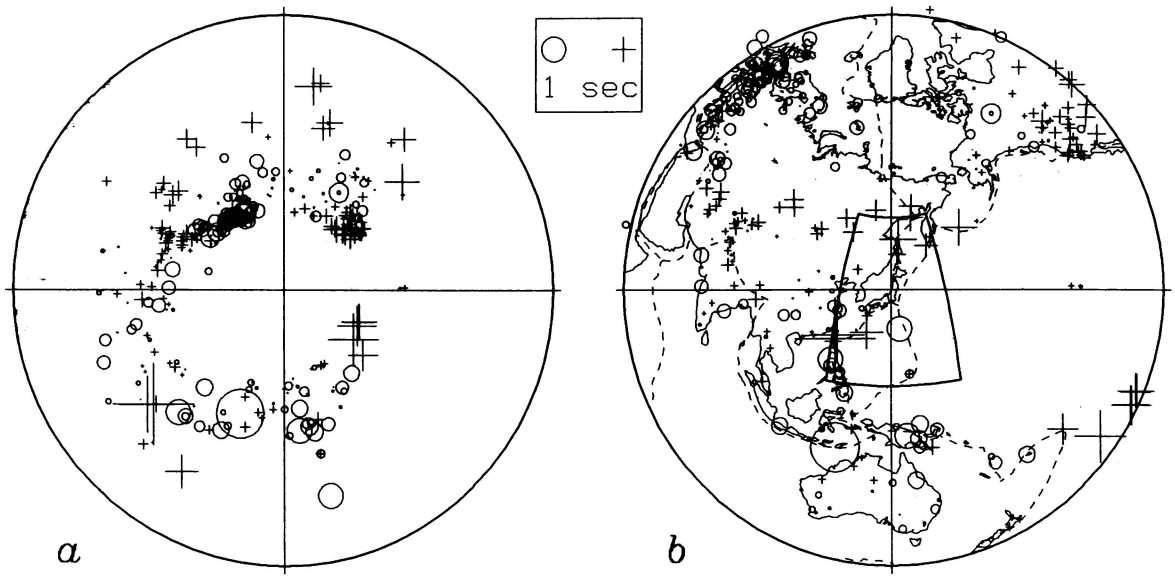

FIG. 2. Station residual averages. The two spheres, a RS (*a*) and a station map (*b*), are centered at 38.6°N, 139.2°E and 411-km depth in the study region (boxed region in *b*). The circumference in *a* corresponds to rays of take-off angle 90°, and in *b* it corresponds to an epicentral distance of 90°. Crosses and circles denote late and early arrivals, respectively, and their sizes correspond to the values of the averages, on the scale given in the box. Each average is constructed at a station by using earthquakes deeper than 300 km in the study region (solid stars in Fig. 1) and represents the teleseismic effect from the region toward the station. These average station residuals are used to correct individual earthquakes for teleseismic effects.

The use of velocity models can be avoided completely in the teleseismic correction by removing station residual averages constructed from earthquakes in the study region. Fig. 2 shows station averages constructed by using 94 events, of focal depth greater than 300 km, from the 145 events in ref. 4. Each station average is the mean of travel-time residuals of at least 20 of these events, representing the teleseismic effect from the study region toward the station. The pattern of the station residual averages is quite robust and is essentially the same as that constructed in ref. 4 based on a different set of events. Station residual averages based on a global earthquake data base, however, contain the near-station contributions but not the deep-mantle teleseismic effects needed here. The station averages shown in Fig. 2 are removed from the residual data as our second type of teleseismic correction.

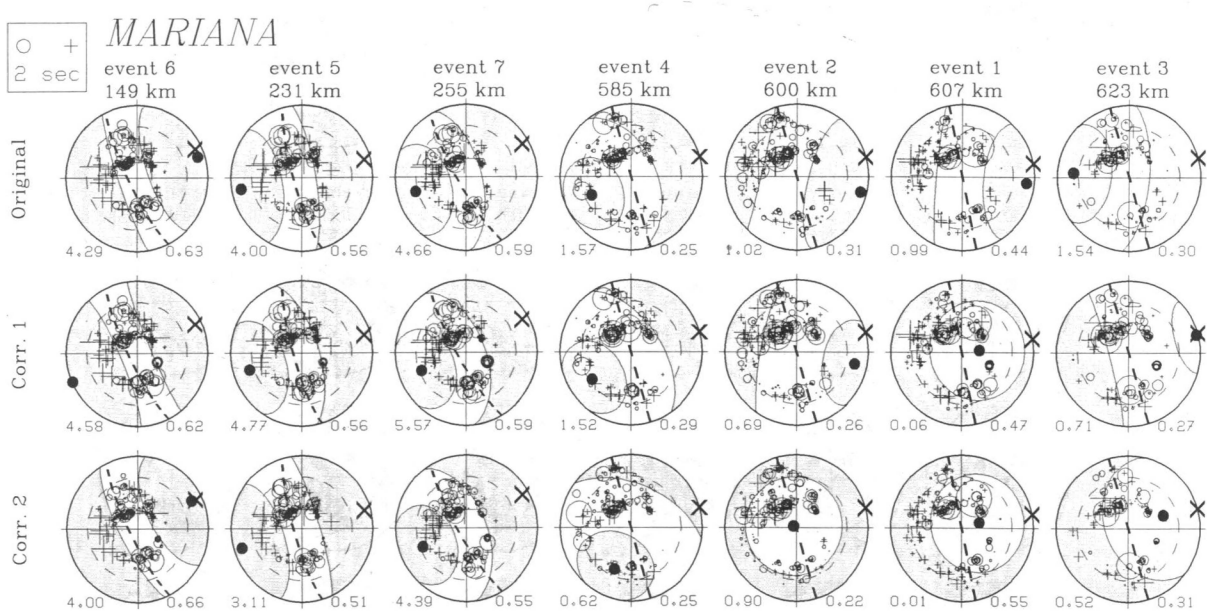

FIG. 3. Fast bands for Mariana events. This and the next three figures display the dominant fast bands in RS in four areas. Spheres in each row are ordered from shallow to deep events. Each column of three spheres represent one event; the original data (after standard corrections and source relocation) and data after each type of teleseismic correction. The circumference and the dashed circle correspond to rays of take-off angle 90° and 60°. Crosses and circles denote late and early residuals. The best-fitting surface of the residuals is displayed; ● is its pole, which is normal to the slab-like band, and the unshaded and shaded areas, respectively, correspond to negative (fast) and positive (slow) regions. The two numbers below are the C_2 value at the left and the correlation coefficient of the fitting at the right. × is the direction normal to the seismicity trend shown by the heavy dashed curve. Fittings for events in this area are generally good, and the results from the two types of corrections are similar. The fast bands generally agree with the trends of seismicity, suggesting that fast regions may exist below the earthquakes. The amplitude of the fast band (C_2 term) and the correlation coefficient decrease from shallow to deep events.

METHOD OF FITTING

The corrected residuals for each event are projected onto the surface of an imaginary sphere at the hypocenter to form a corrected RS. When a fast slab-like band exists on this surface, its amplitude and orientation can be determined by fitting with spherical harmonics of degree 0 to 2. To reduce the effect of slab distortion near the earthquakes, such as a possible kink near the 650-km discontinuity, rays of take-off angle greater than 90° (take off upwards) are excluded.

We fit RS data with a symmetric surface

$$dt(\theta) = C_0 + C_1\cos\theta + C_2\cos 2\theta,$$

where θ is the colatitude with respect to a symmetric axis normal to an assumed band orientation, and C_0, C_1, and C_2 are convertible to spherical harmonic coefficients. Once a direction for the symmetric axis is given, the linear form of the above equation enables a unique determination of the coefficients. The orientation of the best-fitting symmetric axis can be determined quickly by using symmetry properties of the surface.

When the correlation coefficient is smaller than 0.30 or when the value of the C_2 term is smaller than 0.5 s, the fitting is very unstable, indicating that the trend is undeterminable. Two types of surfaces can result from the fitting procedure; a positive C_2 is a fast-band RS and a negative C_2 is a slow-band RS. The magnitude of the band is quantified by the C_2 value. The best-fitting surface shows either a fast or a slow band on RS. We restrict the fitting to positive C_2, since our purpose is to determine the best-fitting fast band. When the C_2 term exceeds about 6 s, it indicates that the data coverage is poor. The fits for most events studied, particularly the shallower ones, are good. We are pretty sure that a fast slab exists beneath the shallow earthquakes, and this suggests that we should be able to detect fast slabs, if they exist, beneath the deeper events.

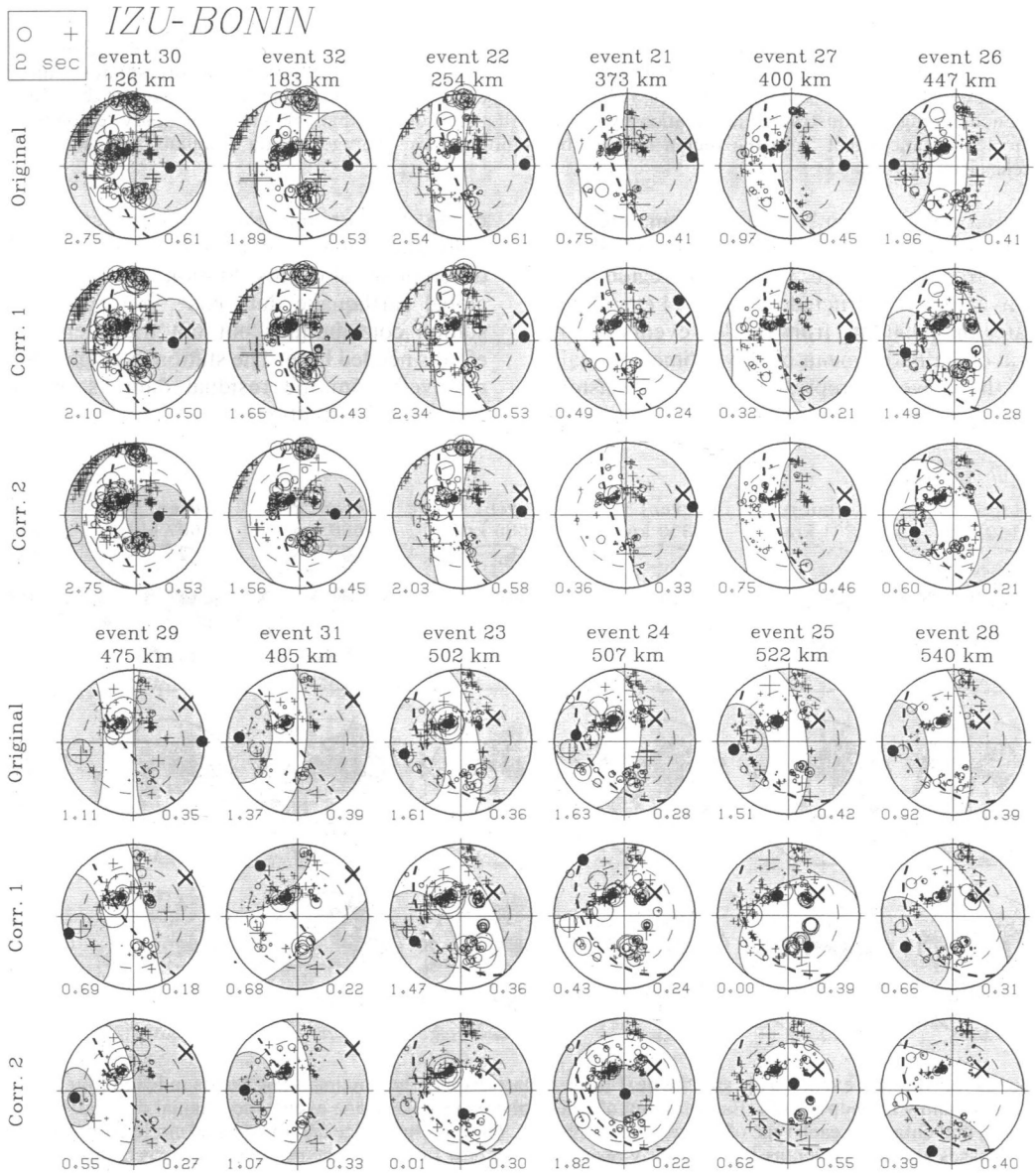

FIG. 4. Fast bands for Izu-Bonin events. Good fits are found for most events in this area. Correlation coefficients are low for events between 300- and 510-km depth, indicating absence of, or poorly resolved, slab-like features. Similar results are found for the two types of corrections for events shallower than 500 km, but the patterns are not consistent for deeper events. The fast bands have orientations close to the seismicity trend only above 500 km.

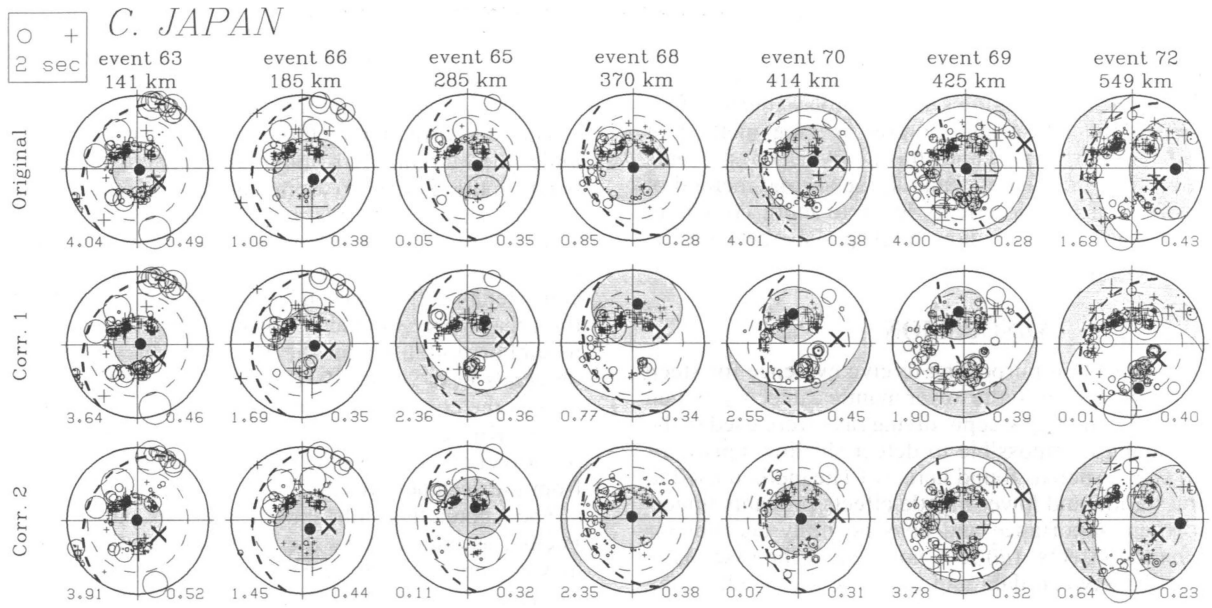

FIG. 5. Fast bands for events in central Japan. Fitting level is generally reasonable, but because the best-fitting fast bands for most events are nearly horizontal, data coverage is quite poor. Results for the two methods are similar. The subhorizontal fast bands are generally associated with shallow dipping seismicity.

RESULTS

The above method is applied to RS data of 33 events that fall in the four shaded areas in Fig. 1. The results, after the two types of corrections, are displayed in Figs. 3–6. Events in the Mariana, Izu-Bonin, and Central Japan areas are generally well fit, and the results from the two corrections are similar. Fast slab-like bands are evident whose trends generally agree with the seismicity trends. The amplitudes and correlation coefficients decrease with depth under the Mariana trench (Fig. 3), where the seismicity-defined slab descends vertically. No such trend is found under Japan (Fig. 5), where the slab (i.e., seismicity) has shallow dip. In fact, the predominant fast band for most deep earthquakes under central Japan is subhorizontal. The implication is that any deep high-velocity slab-like structure there is nearly horizontal.

After teleseismic corrections, the orientations of the fast bands for events under the Izu-Bonin trench (Fig. 4) are consistent with the seismic trends from the surface down to 500 km. Fits are poor for events between 300- and 500-km depth, suggesting either a weak slab-like signal or a distorted slab anomaly. A flattening of the slab at 500- to 550-km depth (9) is consistent with the observations.

The directions of the fast bands in the data from the Kurile trench area are inconsistent and differ from seismicity trends. Recall that we do not limit ourselves to searching for only nearly vertical fast bands—i.e., bands near the trend of the deep seismicity. The fits in this area are poor but generally

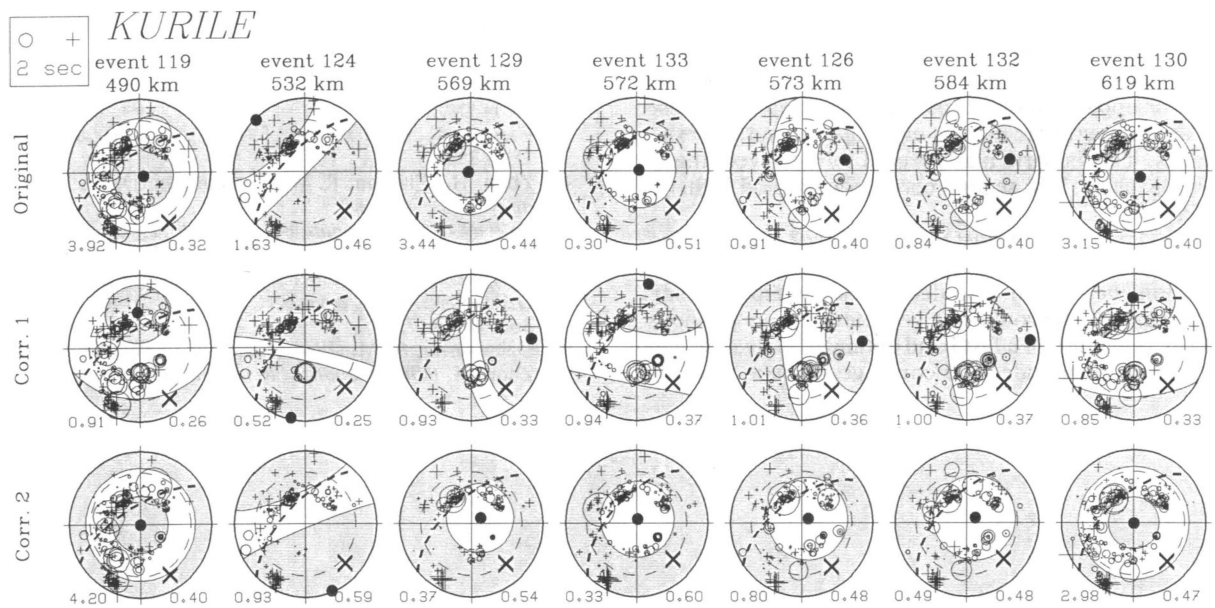

FIG. 6. Fast bands for Kurile events. Correlation coefficients in this area are poor for the first correction but reasonable for the second correction. The orientation of the fast bands is variable. Fast bands for most events differ from the seismicity trend. After the teleseismic correction for Clayton–Comer deep mantle, results for events 129, 126, and 132 in the depth range 370–590 km show north-trending vertical fast bands, and the fast bands are flat or variable for other events. For the second correction method, using teleseismic station averages of regional events, fast bands for all five events deeper than 560 km are horizontal, suggesting that the deep part of the slab is not steeply dipping.

acceptable. After correction for the Clayton–Comer deep-mantle and near-receiver structure, many events in the depth range 375–585 km show fast bands in the trench direction with nearly vertical dip, but dips are flat or variable for other events. When the teleseismic station average method of correction is used, the fast bands for the five deepest events (>560 km) are all horizontal. That is, the second method of correction for teleseismic effects leads to more consistent results, and these imply shallow dipping slabs beneath the deeper earthquakes.

DISCUSSION

Previous studies (1–3) purporting to give evidence for steep slab penetration deep into the lower mantle can be faulted on several grounds: (*i*) Only steeply diving rays were used in the analysis, making it impossible to detect shallow dipping or horizontal slabs, such as found here. (*ii*) The method used to correct for station and lower mantle effects probably underestimated their importance and does not fully account for receiver mantle effects. (*iii*) It is not clear if the essentially perfect match between data and model is the result of the identical heavy smoothing applied to both. (*iv*) There is no criterion of goodness of fit or uniqueness or any test other than the *a priori* model.

In this study we use all mantle-bottoming P waves, from core-grazing to 90° (horizontal) take-off angle, with Jeffreys–Bullen residuals less than 6 s. We correct for teleseismic effects either by using a tomographically determined mantle model or by using average station residuals determined from well-recorded events spread over the whole study area. The wide spacing of the rays in the source region, the variable depths of the events, and the variable trends of slabs mean that, for the residual average at each teleseismic station, upper mantle effects in the source region will tend to cancel out, while coherent deep-mantle and near-receiver effects will tend to accumulate.

One can find a few deep events which give a near-vertical fast band close to the trend of the overlying seismicity. However, these are only a fraction of the total number of events studied and conclusions based on a small number of selected events are not always representative. Note that Creager and Jordan (3) based their deep slab penetration hypothesis on only eight events. Some of these, particularly the deeper ones, do not have an obvious slab signal. The near-receiver upper mantle is not fully corrected out by use of either the tomographic models or the global station residual averages. This is particularly true if the receivers themselves overlie slabs. The second correction method is therefore preferred.

Our method for detecting fast trends does not make *a priori* assumptions about the size, location, or orientation of the fast slab-like anomalies. It can also detect shallow dipping slab-like anomalies which would not be detectable in previous studies. The reliability of a fast band obtained by this method depends on its magnitude, the coverage of data, and the correlation coefficient of the fitting. We have plotted the best-fitting fast trend for every event, although some fits are not very successful (low correlation coefficient) because of limited coverage, and others have rather small C_2 values.

The two correction methods give similar results for events under the Mariana, Izu-Bonin, and Japan trenches. The fast bands in these areas are quite consistent and generally agree with the seismicity trends. In particular, the predominant fast band for most deep earthquakes under Japan is subhorizontal. The results for events under the Izu-Bonin trench are consistent with tomography (9) which showed that the slab in this area steeply subducts to around 500 km and then flattens to subhorizontal. Under the Mariana trench, where the slab descends near vertically, the amplitude of the fast band as well as the correlation decreases with depth. The fast bands for the Kurile events are not well determined. The two types of corrections give results which differ from each other and from the seismicity trend.

The subducting lithospheric slab in parts of the NW Pacific, as indicated by the RS fitting results in this study, may extend below the deepest earthquakes. For events in the Mariana area, where the seismicity is nearly vertical, the RS fast bands, for the shallower events, follow the seismicity trend well, and there is a general decrease in slab signature with depth. Unfortunately, the depth extent of the slab cannot be uniquely determined by the RS method without assuming the magnitude and geometry of the velocity anomalies. Note that the three deepest Mariana events have consistent orientations for the second type of correction (lower row), whereas the first type of correction gives quite different results for a small change in focal depth. The consistent pattern, however, is more like a fast steep cone than a slab.

In conclusion, after correcting for the teleseismic effect, we see only weak evidence for the presence of high-velocity slab-like patterns under the deeper earthquakes and the trends of these features are often shallow dipping or subhorizontal.

This research was supported by National Science Foundation Grants EAR 83-17623 and EAR 85-09350. This is contribution no. 4781 of the Division of Geological and Planetary Sciences, California Institute of Technology.

1. Jordan, T. H. (1977) *J. Geophys.* **43,** 473–496.
2. Creager, K. C. & Jordan, T. H. (1984) *J. Geophys. Res.* **89,** 3031–3049.
3. Creager, K. C. & Jordan, T. H. (1986) *J. Geophys. Res.* **91,** 3573–3580.
4. Zhou, H., Clayton, R. W. & Anderson, D. L. (1989) *J. Geophys. Res.*, in press.
5. *Bulletin of the International Seismological Centre, 1964–1982* (Thatcham, Newbury RG13 4NS, Berkshire, U.K.).
6. Clayton, R. W. & Comer, R. P. (1983) *Eos* **64,** 776.
7. Dziewonski, A. M. & Gilbert, F. (1976) *Geophys. J. R. Astron. Soc.* **44,** 7–17.
8. Dziewonski, A. M. (1984) *J. Geophys. Res.* **89,** 5929–5952.
9. Zhou, H. (1988) *Geophys. Res. Lett.* **15,** 1425–1428.